LA-6188

UC-34c

Issued: January 1977

MASTER

^{4}He(t, t)^{4}He Elastic Scattering: Analyzing Powers and Differential Cross Sections

by

R. A. Hardekopf
Nelson Jarmie
G. G. Ohlsen
R. V. Poore
R. F. Haglund, Jr.
Ronald E. Brown*
P. A. Schmelzbach**
B. D. Anderson†
D. M. Stupin
P. A. Lovoi††

*Visiting Staff Member. University of Minnesota, Minneapolis, MN 55455.
**Long-Term Visiting Staff Member. Eidgenoessische Technische Hochschule, Zürich, Switzerland.
†Guest Scientist. Kent State University, Kent, OH 44242.
††Associated Western Universities, Inc., Graduate Student. ILC Technology, Inc., 164 Commercial Street, Sunnyvale, CA 94086.

los alamos
scientific laboratory
of the University of California
LOS ALAMOS, NEW MEXICO 87545

An Affirmative Action/Equal Opportunity Employer

UNITED STATES
ENERGY RESEARCH AND DEVELOPMENT ADMINISTRATION
CONTRACT W-7405-ENG. 36

Printed in the United States of America. Available from
National Technical Information Service
U.S. Department of Commerce
5285 Port Royal Road
Springfield, VA 22161
Price: Printed Copy $3.50 Microfiche $3.00

This report was prepared as an account of work sponsored by the United States Government. Neither the United States nor the United States Energy Research and Development Administration, nor any of their employees, nor any of their contractors, subcontractors, or their employees, makes any warranty, express or implied, or assumes any legal liability or responsibility for the accuracy, completeness or usefulness of any information, apparatus, product, or process disclosed, or represents that its use would not infringe privately owned rights.

NOTICE
This report was prepared as an account of work sponsored by the United States Government. Neither the United States nor the United States Energy Research and Development Administration, nor any of their employees, nor any of their contractors, subcontractors, or their employees, makes any warranty, express or implied, or assumes any legal liability or responsibility for the accuracy, completeness or usefulness of any information, apparatus, product or process disclosed, or represents that its use would not infringe privately owned rights.

^{4}He(t,t)^{4}He ELASTIC SCATTERING: ANALYZING POWERS AND DIFFERENTIAL CROSS SECTIONS

by

R. A. Hardekopf, Nelson Jarmie, G. G. Ohlsen, R. V. Poore, R. F. Haglund, Jr., Ronald E. Brown, P. A. Schmelzbach, B. D. Anderson, D. M. Stupin, and P. A. Lovoi

ABSTRACT

Analyzing power and differential cross-section results are presented in tabular and graphical form for ^{4}He(t,t)^{4}He elastic scattering from 7- to 14-MeV bombarding energy. The experimental procedure is described for measuring the analyzing powers.

I. INTRODUCTION

This report presents tabulations and graphs of ^{4}He(t,t)^{4}He elastic scattering data obtained recently at the Los Alamos Scientific Laboratory tandem Van de Graaff facility. The analyzing power data result from the first experiment performed with a polarized triton source;[1] the experimental procedure is included for this reason. Details of the differential cross-section experiment are reported elsewhere,[2] but the data from that experiment are included here for completeness.

II. EXPERIMENTAL EQUIPMENT AND PROCEDURE FOR ANALYZING POWER MEASUREMENTS

The analyzing power experiment was performed with a polarized triton beam striking a ^{4}He gas target. Two detectors at symmetric angles each simultaneously monitored scattered tritons and recoil alphas to collect data from which the analyzing powers were obtained.

The polarized triton beam was focused onto the target at the center of the supercube[3,4] scattering chamber. The beamline plan is shown in Fig. 1. Entrance slits to the chamber (2.54 mm^2) were located 60.6 cm from the center of the target. A set of antiscatter slits (3.05 mm^2) were located 40.3 cm from the target center. A circular collimator 2.54 mm in diameter preceded the 2.5-μm-thick target entrance foil, and antiscatter baffles followed it. After passing through the target, the beam was collected on the chamber exit slits 65.6 cm from target center as well as on the Faraday cup which followed. A beam position indicator simultaneously displayed the current intercepted by the first set of entrance slits and by the exit slits. Beam position was maintained throughout the experiment by keeping the current on these slits balanced in the left-right and up-down directions. Currents on the exit slits were added to the Faraday cup current, and the total was recorded by a current integrator.

The target, shown schematically in Fig. 2, was a 10-cm-diam cylindrical gas cell pressurized with ^{4}He to 300 torr and covered at first with 2.5-μm-thick Havar foil, then later with 6.3-μm-thick Kapton plastic film. For measurements with the Kapton film, a 3-ℓ buffer was attached to the gas-cell filler tube to compensate for diffusion losses through the film.

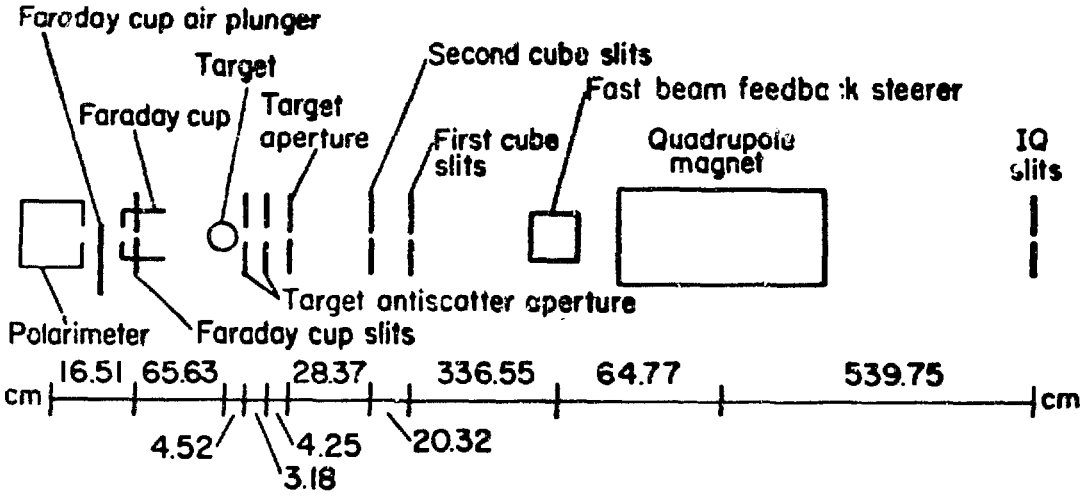

Fig. 1.
Supercube scattering chamber beamline plan (not to scale). Slit sizes are given in the text

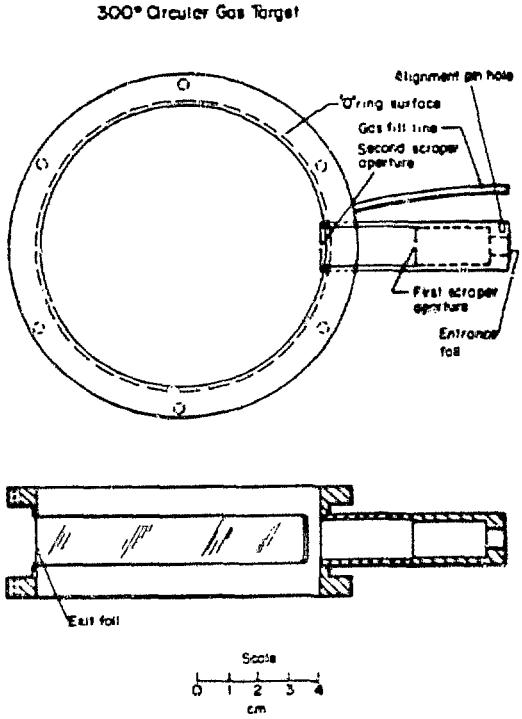

Fig. 2.
Schematic of 300° circular target. The target was pressurized to 300 torr with ^{4}He.

Two detector telescopes viewed the target at equal angles left and right of the beam axis. Figure 3 shows the detector snouts used with the gas target. Each detector collimator consisted of a front rectangular slit 5.1 cm from the target center and a rear rectangular slit 24.1 cm from the target center. Both collimator apertures were 3.33 mm wide by 11.4 mm high, giving an angular resolution of 1.0°, full width at half maximum (FWHM). Mean scattering angles were determined to ±0.05°. Further details on the collimators, antiscatter slits, and supercube hardware can be found in Ref. 4.

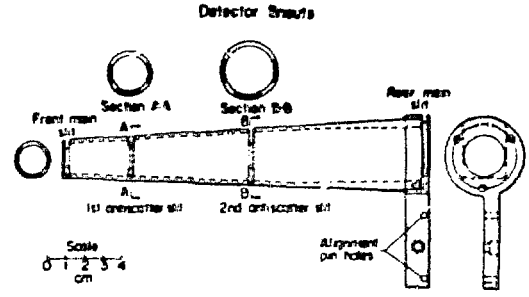

Fig. 3.
Detector snouts used to hold collimators for gas target geometry. The dimensions of the collimator slits are given in the text.

Each counter telescope contained a 48-μm-thick-thick ΔE detector and a 1000-μm-thick E detector. For those events which gave rise to a ΔE-E coincidence, linear ΔE and E signals were sent to analog-to-digital converters (ADCs) and stored in an on-line computer. Mass identification was performed by computer processing; events resulting from tritons and recoil alpha particles were stored in separate memory blocks. Alpha particles penetrated ΔE detectors only for higher energies and forward angles. Therefore, ΔE singles spectra were simultaneously stored by means of separate ADCs. Most alpha particle data were obtained in this *singles* mode.

Peak sums were obtained on-line by setting relatively narrow gates on the peaks. A visually satisfactory linear background line was set by means of a wider "background gate," and the linear background under the peak was subtracted in the analysis routine. For most of the data, the background counts thus obtained were much less than 1% of the peak sums. For some of the data where alpha particles were detected in *singles* mode, background counts approached 3%. Even in these cases the analyzing power calculations, with and without background correction differed by less than statistical error. Corrected counts were used for the final tabulation.

The data acquisition sequence for each angle consisted of runs of equal integrated charge for triton beam polarization in the up-down directions. Beam polarization P_Q was determined by averaging quench-ratio[5] results obtained before and after each run. These results were determined from the accelerated beam by a computer routine that measures, with a digital picoammeter, the ratio Q of normal beam current to quenched beam current and calculates

$$P_Q = 1 - \frac{1}{Q} .$$

Two measurements of P_Q were made each time the routine was called; their average was stored in the computer. In this manner, eight P_Q values were averaged for a spin-up, spin-down sequence. The final average P_Q was used in calculating the analyzing power. Accuracy of the quench-ratio technique for triton beam polarization was one of the results determined in this experiment: it was found to be accurate to within ±0.010 (Ref. 6).

Analyzing powers A_y were calculated from the geometric average of left (L) and right (R) detector yields for the two runs:

$$r = \left(\frac{L\uparrow R\downarrow}{R\uparrow L\downarrow}\right)^{1/2}$$

$$A_y = \frac{1}{P_Q}\left[\frac{r-1}{r+1}\right]$$

where the arrows indicate spin-up and spin-down beam polarizations. This method cancels the effects of differences in detector efficiency and of errors in current integration.[7] Data acquisition and processing, quench-ratio measurements, spin-direction control of the polarized source, A_y calculations, and detector angle changes in the scattering chamber were entirely under computer control. This freed the experimenter to concentrate on setting foreground and background gates in the spectra and to monitor the data acquisition.

An important correction is necessary to both the analyzing power and cross-section data when there is a combination of a large curvature in the angular distribution and a significant multiple scattering of the detected particles in the target exit foil. In this case, the particles multiply-scattered into and away from the detector did not completely compensate each other. The effect was especially serious for the sharp peaks at large c.m. angles where alpha particles were detected. With a Havar foil target, corrections as large as 14% in the cross section and 0.1 to 0.2 in the analyzing power were necessary. Much of the A_y data and some of the cross-section data, where alphas were detected, were rerun with the target gas contained by a Kapton film. Approximate correction formulas[8] and a Monte Carlo program[9] were developed and used to make corrections (usually less than 3%) to the cross-section data. The results of the runs with a Kapton target, the formulas, and the Monte Carlo program were consistent. Larger-than-normal errors seen in parts of the data are the result of the above problem.

III. ANALYZING POWER DATA

Complete angular distributions of the analyzing powers were obtained at three energies: 8.785, 10.815, and 12.250 MeV. Partial distributions were obtained at four other energies from 10.2-11.7 MeV near the angular region where A_y approaches its minimum possible value of -1. These data have been discussed in Ref. 10. In addition to an extensive excitation function at $\Theta_{lab} = 28.5°$, some excitation function data were obtained at $\Theta_{lab} = 35.0°$ near the energy where a Wigner Cusp effect[2,11,12] was expected.

Energy of the bombarding beam was known to ±15 keV with a FWHM spread of 40 keV including the effects of foil and target-gas straggling and machine energy resolution. The relative energy of adjacent runs in an excitation function is accurate to ±5 keV.

Analyzing power data obtained with the polarized triton beam are summarized in Tables I and II. Numerical data are tabulated in Appendix A. Figures 4-6 show the polarization data in graphical form. Shown for comparison in Fig. 5 are data from Ref. 13.

The relative accuracy of the data is generally better than ±0.020, and much of it is better than ±0.007. Relative errors listed in Appendix A are primarily statistical, although when the statistical error was less than ±0.007, we took this value as a lower limit. The limit results from our knowledge of the background and from our observation of maximum fluctuation in quench-ratio determinations of beam polarization. It also derives from our observations over many years of the reproducibility of proton analyzing power data taken with similar techniques. We believe the scale error for these measurements (i.e., the amount they could be renormalized in order to minimize χ^2 in a search) to be 1%. This is a multiplicative factor based on long-term observations of the quench-ratio accuracy under varying operating conditions of the polarized source.

The data at 10.200, 11.100, 11.390, and 11.700 MeV near the $A_y = -1$ point (see Fig. 6) have not been corrected for multiple scattering (since the curvatures are obscure), nor repeated with a Kapton target. The points that might have a significant correction are in those at 100° c.m. and larger. This will not affect the conclusions of the analyzing power calibration in Ref. 10, but these particular data should be used with caution in a numerical analysis.

A preliminary report of the polarization data has been presented.[8,10,14]

TABLE I

RANGE OF ANGULAR DISTRIBUTIONS FOR $A_y(\Theta)$

Energy (MeV)	$\Theta_{c.m.}$ (deg)	Data Points
8.785	26-150	31
10.200	61-110	12
10.815	28-148	58
11.100	56-115	14
11.390	61-110	12
11.700	61-110	12
12.250	26-150	30

TABLE II

RANGE OF EXCITATION FUNCTIONS FOR $A_y(\Theta)$

Energy (MeV)	Θ_{lab} (deg)	$\Theta_{c.m.}$ (deg)	Data Points
7.000-14.200	28.5[a]	49.6	60
7.000-14.200	28.5[b]	123.0	15
8.200-8.870	35.0[a]	60.6	12
8.200-8.870	35.0[b]	110.0	12

[a]Tritons.
[b]Alphas.

IV. DIFFERENTIAL CROSS SECTION DATA

The differential cross-section data[3] included in this report were taken with an unpolarized triton

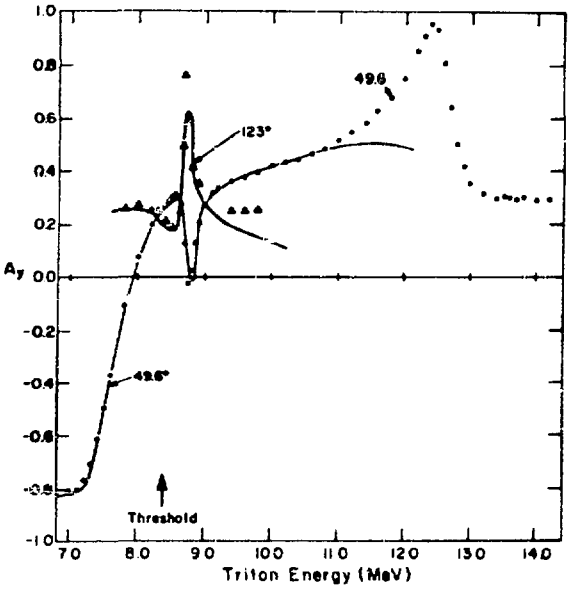

Fig. 4.
Excitation function for the $^4He(t,t)^4He$ analyzing power.

beam in an Ortec* 60-cm scattering chamber. Relative and scale errors are listed in the tabulations. Energy errors are the same as those discussed with the analyzing power data. Angular width of the double-slit system was 0.3° FWHM, and the final accuracy of the measured angle was ±0.03°.

Tables III and IV summarize the differential cross-section data; complete tables are provided in Appendix B. Figures 7 and 8 show the data in graphical form.

V. DISCUSSION

Experimental procedures and numerical data have been reported for accurate measurements of the $^4He(t,t)^4He$ reaction from 7 to 14 MeV. Both the analyzing power data and differential cross-section data are presently being used (with data from other laboratories in both the alpha + triton and ^6Li + neutron channels) in an R-matrix analysis of the ^7Li system.[16] The solid lines in Figs. 4, 5, 7, and 8 are preliminary R-matrix predictions which were obtained without using a complete set of the present

*Ortec Inc., Oak Ridge, TN 37830.

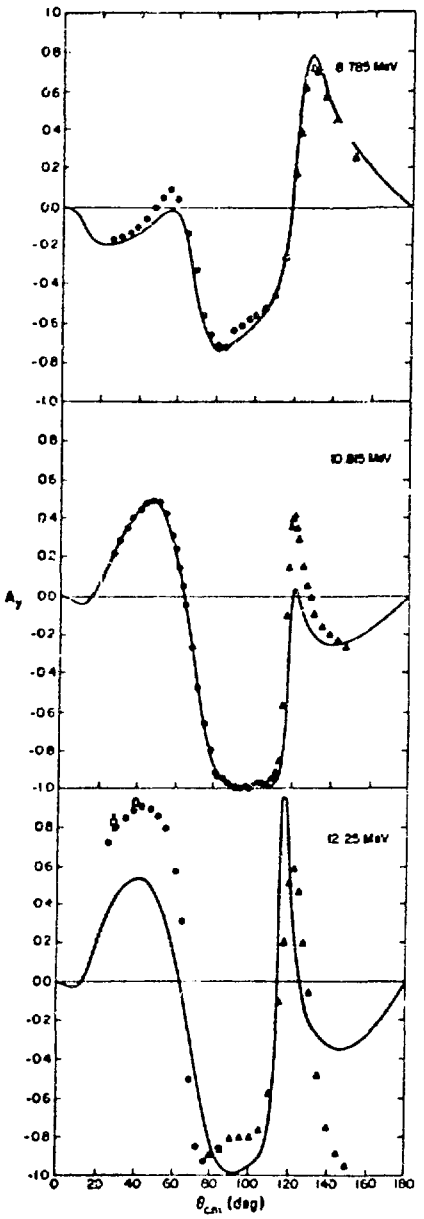

Fig. 5.
Angular distributions of the analyzing power for $^4He(t,t)^4He$ elastic scattering. The open square points at low angles at 12.25 MeV are from the double-scattering measurements of Keaton et al. (Ref. 13).

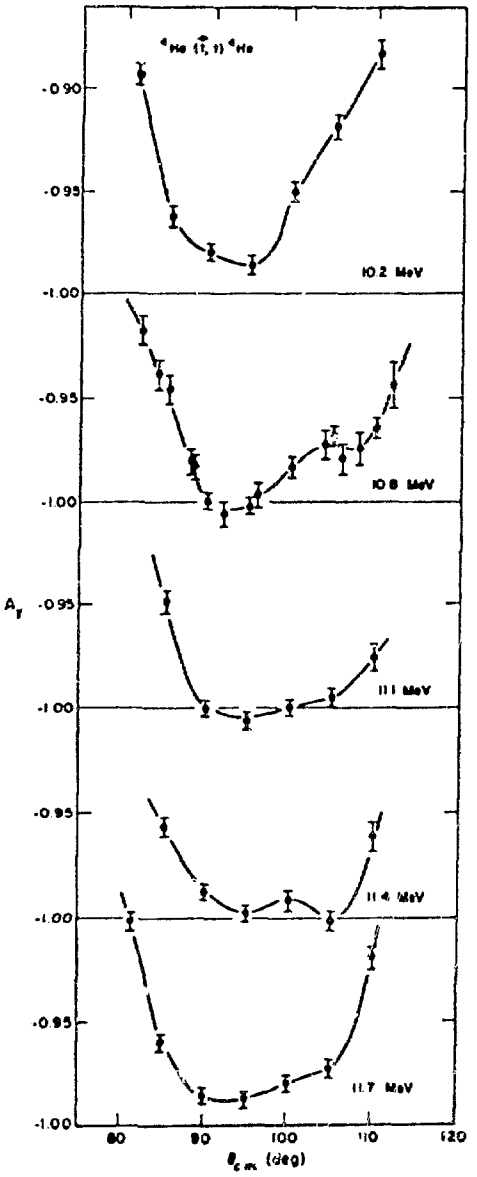

Fig. 6.
Angular distributions of the analyzing power for ^{4}He(t,t)^{4}He elastic scattering near $A_y = -1$. Solid lines only connect data points as a visual guide.

data, in particular the final analyzing powers. The indication is that both the cross sections and the analyzing powers will have a strong influence on the fit.

TABLE III

RANGE OF ANGULAR DISTRIBUTIONS FOR σ (Θ)

Energy (MeV)	$\Theta_{c.m.}$ (deg)	Data Points
8.230	22-155	22
8.580	22-155	18
8.790	22-155	17
8.980	22-155	24
9.880	22-155	27
12.000	22-155	17

TABLE IV

RANGE OF EXCITATION FUNCTIONS FOR σ (Θ)

(Energy = 7.600-10.000 MeV)

Θ_{lab} (deg)	$\Theta_{c.m.}$ (deg)	Data Points
15.0[a]	26.3	21
15.0[b]	150.0	21
28.5[a]	49.6	22
28.5[b]	123.0	21
40.0[a]	69.0	21

[a]Tritons.
[b]Alphas.

Although it is not apparent in the figures as drawn, a careful study of the data and the R-matrix fit does indicate a slight anomaly near 8.4 MeV where a Wigner Cusp[11,12] is expected. The effect is certainly not very marked, and further precision experiments should be done if the nature of the cusp is to be explored.

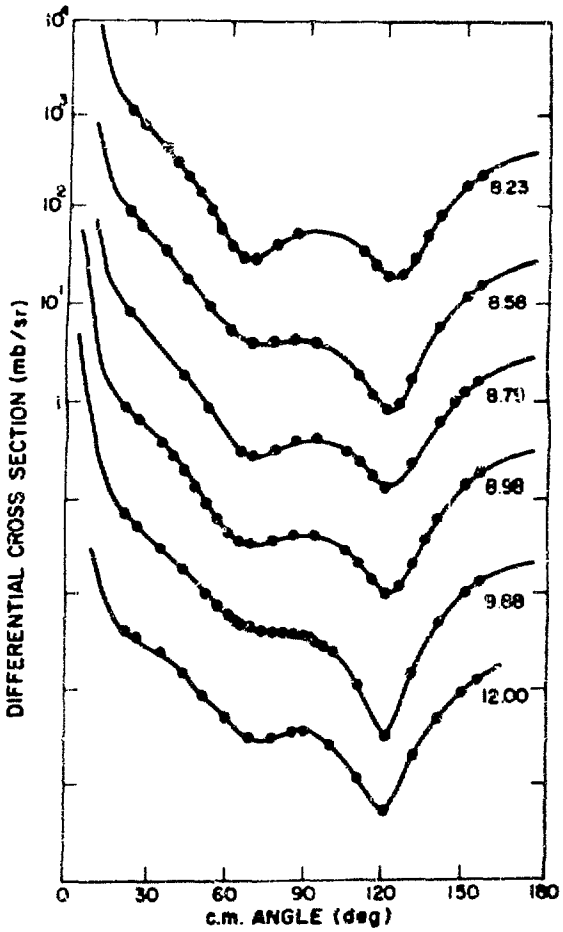

Fig. 7.
Angular distributions of the differential cross section for $^4He(t,t)^4He$ elastic scattering.

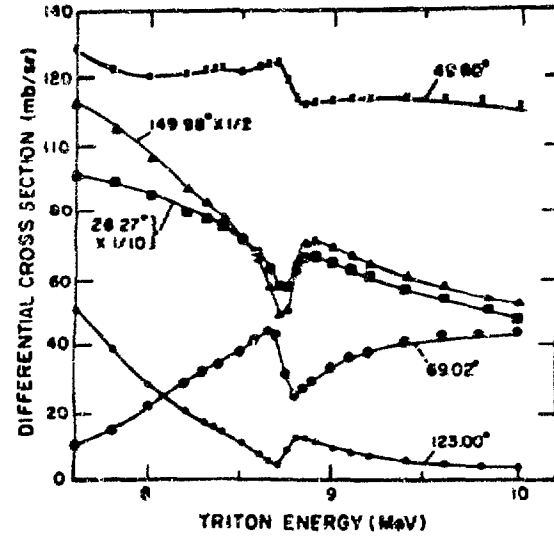

Fig. 8.
Excitation functions for the $^4He(t,t)^4He$ differential cross section

ACKNOWLEDGMENTS

It is a pleasure to acknowledge the assistance of Louis Morrison in the construction of the polarized triton source and the experimental apparatus. We are also indebted to D. C. Dodder and G. M. Hale for providing the predictions of their R-matrix analysis before publication. H. C. Britt, J. Sunier, and R. J. Barrett helped greatly taking data in the cross-section experiments.

REFERENCES

1. R. A. Hardekopf, "Operation of the LASL Polarized Triton Source," Proc. 4th Int. Symp. Polariz. Phenom. Nucl. React., Zürich, 25-29 August 1975 (Birkhauser Verlag, Basel, 1976), p. 865.

2. N. Jarmie, G. G. Ohlsen, P. A. Lovoi, D. M. Stupin, R. A. Hardekopf, B. D. Anderson, J. W. Sunier, R. V. Poore, R. J. Barrett, G. M. Hale, and D. C. Dodder, "Elastic Scattering of 7-12 MeV Tritons by Alpha Particles," to be published. Abstract in Bull. Am. Phys. Soc. **20**, 596 (1975). See Phys. Rev. C3, 10 (1971) for experimental arrangement.

3. G. G. Ohlsen and P. A. Lovoi, "The 'Supercube' Scattering Chamber for Spin 1/2 and Spin 1 Analyzing Power Measurements," Proc. 4th Int. Symp. Polariz. Phenom. Nucl. React., Zürich, 25-29 August 1975 (Birkhäuser Verlag, Basel, 1976), p. 907.

4. P. A. Lovoi, "Proton-Proton Analyzing Power Measurements at 16 MeV," Ph.D. Dissertation, Univ. of New Mexico, 1975. Also Los Alamos Scientific Laboratory report LA-6041-T (September 1975).

5. G. G. Ohlsen, J. L. McKibben, G. P. Lawrence, P. W. Keaton, Jr., and D. D. Armstrong, "Precise Proton-Polarization Standards Determined with a Lamb-Shift Ion Source Incorporating a Nuclear Spin Filter," Phys. Rev. Lett. **27**, 599 (1971).

6. R. A. Hardekopf, G. G. Ohlsen, R. V. Poore, and N. Jarmie, "Calibration of a Polarized Triton Beam," Proc. 4th Int. Symp. Polariz. Phenom. Nucl. React., Zürich, 25-29 August 1975 (Birkhäuser Verlag, Basel, 1976), p. 903.

7. G. G. Ohlsen and P. W. Keaton, Jr., "Techniques for Measurement of Spin-1/2 and Spin-1 Polarization Analyzing Tensors," Nucl. Instrum. Methods **109**, 42 (1973).

8. N. Jarmie, R. E. Brown, P. A. Schmelzbach, and R. F. Haglund, Jr., to be published.

9. Nelson Jarmie, J. H. Jett, and A. C. Niethammer, "SPANDY - A Monte Carlo Program for Simulation of Gas Target Scattering Geometry," Los Alamos Scientific Laboratory report LA-6611, to be published.

10. R. A. Hardekopf, G. G. Ohlsen, R. V. Poore, and N. Jarmie, "Location of a Polarization Extremum in Triton-Alpha Scattering and its Application to a New Polarized Triton Source," Phys. Rev. C**13**, 2127 (1976).

11. N. Jarmie and R. C. Allen, "T(p,p)T Near the T(p,n)^{3}He Threshold," Phys. Rev. **114**, 176 (1959).

12. E. P. Wigner, "On the Behavior of Cross Sections Near Thresholds," Phys. Rev. **73**, 1002 (1948).

13. P. W. Keaton, Jr., D. D. Armstrong, and L. R. Veeser, "Polarization of Tritons Scattered from ^{3}He," Phys. Rev. Lett. **20**, 1392 (1968).

14. R. A. Hardekopf, N. Jarmie, G. G. Ohlsen, and R. V. Poore, "Analyzing Power for ^{3}He(t,t)^{3}He Elastic Scattering," Proc. 4th Int. Symp. Polariz. Phenom. Nucl. React., Zürich, 25-29 August 1975 (Birkhäuser Verlag, Basel, 1976), p. 579.

15. G. M. Hale, "R-Matrix Analysis of the Light Element Standards," in *Nuclear Cross-Sections and Technology*, Nat. Bur. Stand. Spec. Publ. 425, Vol. 1 (1975), p. 302.

APPENDIX A

ANALYZING POWER A_y FOR $^4He(t,t)^4He$

$^4He(t,t)^4He$ 8.785 MeV

θ_{lab} (deg)	θ_{cm} (deg)	$A_y(\theta)$	Error
15.0	26.3	-0.169	0.007
17.5	30.6	-0.157	0.007
20.0	35.0	-0.132	0.007
22.5	39.3	-0.103	0.007
25.0	43.6	-0.055	0.007
27.5	47.9	-0.003	0.007
30.0	52.2	0.045	0.007
32.5	56.4	0.090	0.007
35.0	60.6	0.045	0.007
37.5	64.8	-0.134	0.007
40.0	69.0	-0.332	0.007
42.5	73.2	-0.559	0.007
45.0	77.2	-0.664	0.007
47.5	81.3	-0.715	0.007
50.0	85.3	-0.720	0.007
52.5	89.3	-0.634	0.007
55.0	93.2	-0.615	0.007
57.5	97.0	-0.575	0.011
40.0[a]	100.0	-0.563	0.007
37.5[a]	105.0	-0.526	0.007
35.0[a]	110.0	-0.458	0.007
32.5[a]	115.0	-0.258	0.011
30.0[a]	120.0	0.168	0.010
29.0[a]	122.0	0.388	0.009
27.5[a]	125.0	0.627	0.008
26.0[a]	128.0	0.717	0.007
25.0[a]	130.0	0.710	0.007
22.5[a]	135.0	0.575	0.007
20.0[a]	140.0	0.446	0.007
17.5[a]	145.0	0.350	0.007
15.0[a]	150.0	0.257	0.007

[a] alpha particle detected.

$^4He(t,t)^4He$ 10.200 MeV

θ_{lab} (deg)	θ_{cm} (deg)	$A_y(\theta)$	Error
35.0	60.6	0.197	0.007
37.5	64.8	-0.039	0.007
40.0	69.0	-0.312	0.007
42.5	73.2	-0.575	0.007
45.0	77.2	-0.778	0.007
47.5	81.3	-0.894	0.007
50.0	85.3	-0.963	0.007
45.0[a]	90.0	-0.980	0.007
42.5[a]	95.0	-0.986	0.007
40.0[a]	100.0	-0.951	0.007
37.5[a]	105.0	-0.919	0.007
35.0[a]	110.0	-0.884	0.007

[a] alpha particle detected.

$^4He(t,t)^4He$ 10.815 MeV

θ_{lab} (deg)	θ_{cm} (deg)	$A_y(\theta)$	Error
16.0	28.0	0.216	0.007
18.0	31.5	0.279	0.007
20.0	35.0	0.340	0.007
22.0	38.4	0.400	0.007
24.0	41.9	0.444	0.007
26.0	45.3	0.478	0.007
28.0	48.8	0.490	0.007
30.0	52.2	0.477	0.007
32.0	55.6	0.421	0.007
34.0	59.0	0.309	0.007
35.0	60.6	0.237	0.007
36.0	62.3	0.143	0.007
37.0	64.0	0.052	0.007
37.5	64.8	0.003	0.007
38.0	65.7	-0.045	0.008
40.0	69.0	-0.267	0.007
42.0	72.3	-0.480	0.009
42.5	73.2	-0.531	0.007
44.0	75.6	-0.664	0.008
45.0	77.2	-0.732	0.007
46.0	78.9	-0.799	0.008
47.5	81.3	-0.869	0.007
48.0	82.1	-0.918	0.007
48.0[a]	84.0	-0.939	0.007
50.0	85.3	-0.946	0.007
46.0[a]	88.0	-0.981	0.007
52.0	88.5	-0.984	0.007
45.0[a]	90.0	-0.999	0.007
54.0	91.6	-0.990	0.007
44.0[a]	92.0	-1.006	0.007
56.0	94.7	-1.004	0.007
42.5[a]	95.0	-1.002	0.007
42.0[a]	96.0	-0.997	0.007
58.0	97.8	-1.002	0.008
40.0[a]	100.0	-0.979	0.010
38.0[a]	104.0	-0.958	0.012
37.5[a]	105.0	-0.968	0.007
37.0[a]	106.0	-0.980	0.007
36.0[a]	108.0	-0.971	0.010
35.0[a]	110.0	-0.965	0.007
34.0[a]	112.0	-0.907	0.012
33.0[a]	114.0	-0.855	0.013
32.0[a]	116.0	-0.566	0.018
31.0[a]	118.0	-0.090	0.023
30.5[a]	119.0	0.158	0.020
30.0[a]	120.0	0.375	0.020
29.5[a]	121.0	0.420	0.018
29.0[a]	122.0	0.430	0.016
28.5[a]	123.0	0.369	0.015
28.0[a]	124.0	0.302	0.013
27.0[a]	126.0	0.150	0.013
26.0[a]	128.0	0.056	0.012
25.5[a]	129.0	0.004	0.009
24.0[a]	132.0	-0.089	0.008
22.0[a]	136.0	-0.174	0.008
20.0[a]	140.0	-0.204	0.010
18.0[a]	144.0	-0.232	0.010
16.0[a]	148.0	-0.266	0.010

[a] alpha particle detected.

$^4He(t,t)^4He$ 11.100 MeV

θ_{lab} (deg)	$\theta_{cm.}$ (deg)	$A_y(\theta)$	Error
32.5	56.4	0.432	0.007
35.0	60.6	0.270	0.007
37.5	64.8	0.030	0.007
40.0	69.0	-0.265	0.007
42.5	73.2	-0.526	0.007
45.0	77.2	-0.737	0.007
47.5	81.3	-0.881	0.007
50.0	85.3	-0.948	0.007
45.0[a]	90.0	-1.000	0.007
42.5[a]	95.0	-1.006	0.007
40.0[a]	100.0	-1.000	0.007
37.5[a]	105.0	-0.995	0.007
35.0[a]	110.0	-0.975	0.007
32.5[a]	115.0	-0.720	0.013

[a] alpha particle detected.

$^4He(t,t)^4He$ 11.700 MeV

θ_{lab} (deg)	$\theta_{cm.}$ (deg)	$A_y(\theta)$	Error
35.0	60.6	0.348	0.007
37.5	64.8	0.069	0.007
40.0	69.0	-0.269	0.007
42.5	73.2	-0.579	0.007
45.0	77.2	-0.795	0.007
47.5	81.3	-0.902	0.007
47.5[a]	85.0	-0.960	0.007
45.0[a]	90.0	-0.986	0.007
42.5[a]	95.0	-0.988	0.007
40.0[a]	100.0	-0.981	0.007
37.5[a]	105.0	-0.973	0.007
35.0[a]	110.0	-0.920	0.007

[a] alpha particle detected.

$^4He(t,t)^4He$ 11.390 MeV

θ_{lab} (deg)	$\theta_{cm.}$ (deg)	$A_y(\theta)$	Error
35.0	60.6	0.320	0.007
37.5	64.8	0.051	0.007
40.0	69.0	-0.246	0.007
42.5	73.2	-0.537	0.007
45.0	77.2	-0.750	0.007
47.5	81.3	-0.890	0.007
50.0	85.3	-0.957	0.007
45.0[a]	90.0	-0.988	0.007
42.5[a]	95.0	-0.998	0.007
40.0[a]	100.0	-0.992	0.007
37.5[a]	105.0	-1.002	0.007
35.0[a]	110.0	-0.962	0.008

[a] alpha particle detected.

$^4He(t,t)^4He$ 12.250 MeV

θ_{lab} (deg)	$\theta_{cm.}$ (deg)	$A_y(\theta)$	Error
15.0	26.3	0.727	0.007
17.5	30.6	0.801	0.007
20.0	35.0	0.851	0.007
22.5	39.3	0.886	0.007
25.0	43.5	0.909	0.007
27.5	47.9	0.896	0.007
30.0	52.2	0.867	0.007
32.5	56.4	0.795	0.007
35.0	60.6	0.578	0.007
37.5	64.8	0.124	0.007
40.0	69.0	-0.505	0.008
42.5	73.2	-0.851	0.007
45.0	77.2	-0.933	0.007
47.5	81.3	-0.895	0.007
47.5[a]	85.0	-0.873	0.007
45.0[a]	90.0	-0.819	0.009
42.5[a]	95.0	-0.810	0.008
40.0[a]	100.0	-0.806	0.007
37.5[a]	105.0	-0.772	0.009
35.0[a]	110.0	-0.580	0.009
32.5[a]	115.0	-0.117	0.009
31.25[a]	117.5	0.202	0.010
30.0[a]	120.0	0.512	0.009
28.75[a]	122.5	0.591	0.009
27.5[a]	125.0	0.467	0.008
26.25[a]	127.5	0.197	0.008
25.0[a]	130.0	-0.062	0.008
22.5[a]	135.0	-0.481	0.007
20.0[a]	140.0	-0.746	0.007
17.5[a]	145.0	-0.889	0.007
15.0[a]	150.0	-0.950	0.007

[a] alpha particle detected.

$^4He(t,t)^4He$

Excitation Function θ_{lab} = 28.5 deg

E_t (MeV)	tritons $\theta_{cm.}$ = 49.6 deg $A_y(\theta)$	Error	alphas $\theta_{cm.}$ = 123.0 deg $A_y(\theta)$	Error
7.000	-0.804	0.007		
7.100	-0.802	0.007		
7.200	-0.767	0.007		
7.300	-0.706	0.007		
7.400	-0.616	0.007		
7.500	-0.501	0.007		
7.600	-0.374	0.007		
7.800	-0.108	0.007	0.273	0.008
8.000	0.073	0.007	0.279	0.008
8.200	0.202	0.007	0.253	0.008
8.300	0.242	0.007	0.253	0.008
8.350	0.261	0.007		
8.375	0.271	0.007		
8.400	0.268	0.007	0.214	0.008
8.425	0.279	0.007		
8.450	0.288	0.007		
8.475	0.294	0.007		
8.500	0.304	0.007	0.191	0.010
8.550	0.310	0.007		
8.600	0.299	0.007	0.254	0.013
8.650	0.277	0.007	0.492	0.011
8.700	0.126	0.007	0.770	0.011
8.750	-0.023	0.007	0.596	0.011
8.800	0.024	0.007	0.431	0.011
8.850	0.131	0.007		
8.900	0.208	0.007	0.358	0.012
9.000	0.278	0.007		
9.100	0.314	0.007		
9.200	0.338	0.007		
9.400	0.365	0.007	0.257	0.013
9.600	0.377	0.007	0.269	0.014
9.800	0.395	0.007	0.272	0.017
10.000	0.413	0.007		
10.200	0.427	0.007		
10.400	0.440	0.007		
10.600	0.463	0.007		
10.800	0.485	0.007		
11.000	0.515	0.007		
11.200	0.548	0.007		
11.400	0.585	0.007		
11.600	0.633	0.007		
11.800	0.681	0.007		
12.000	0.748	0.007		
12.200	0.848	0.007		
12.300	0.910	0.007		
12.400	0.952	0.007		
12.500	0.933	0.007		
12.600	0.804	0.007		
12.700	0.642	0.007		
12.800	0.503	0.007		
12.900	0.416	0.007		
13.000	0.356	0.007		
13.200	0.316	0.007		
13.400	0.299	0.007		
13.500	0.306	0.007		
13.600	0.304	0.007		
13.700	0.294	0.007		
13.800	0.307	0.007		
14.000	0.289	0.007		
14.200	0.293	0.007		

$^4He(t,t)^4He$

Excitation Function θ_{lab} = 35.0 deg

E_t (MeV)	tritons $\theta_{cm.}$ = 60.6 deg $A_y(\theta)$	Error	alphas $\theta_{cm.}$ = 110.0 deg $A_y(\theta)$	Error
8.200	0.212	0.008	-0.398	0.010
8.300	0.202	0.008	-0.420	0.010
8.350	0.191	0.007	-0.435	0.010
8.375	0.190	0.007	-0.447	0.010
8.400	0.182	0.007	-0.457	0.010
8.425	0.178	0.007	-0.476	0.010
8.450	0.182	0.007	-0.482	0.010
8.475	0.181	0.007	-0.500	0.010
8.500	0.185	0.007	-0.502	0.010
8.550	0.161	0.007	-0.548	0.010
8.600	0.145	0.007	-0.608	0.010
8.700	0.063	0.007	-0.642	0.010

APPENDIX B

DIFFERENTIAL CROSS SECTIONS $\sigma(\theta)$ FOR $^4He(t,t)^4He$

$^4He(t,t)^4He$ 8.230 MeV

Scale Error = 0.40%

θ_{lab} (deg)	$(\theta)_{lab}$ (mb/sr)	$\theta_{c.m.}$ (deg)	$\sigma(\theta)_{c.m.}$ (mb/sr)	Rel. Error (%)
12.50	3247.0	21.90	1078.0	0.60
15.00	2364.0	26.27	793.1	0.40
20.00	1275.0	34.96	439.1	0.40
22.50	900.5	39.29	314.9	0.40
25.00	613.7	43.60	218.5	0.40
27.50	400.7	47.89	145.5	0.40
30.00	251.0	52.17	93.21	0.45
32.50	156.1	56.42	59.34	0.50
35.00	100.60	60.65	39.27	0.60
37.50	77.04	64.84	30.96	0.60
40.00	72.79	69.01	30.19	0.60
45.00	92.80	77.24	41.28	0.50
50.00	111.1	85.30	53.61	0.70
35.00[a]	115.7	109.97	35.31	2.0
32.50[a]	87.84	114.97	26.03	0.9
30.00[a]	68.98	119.97	19.90	0.9
27.50[a]	71.68	124.97	20.19	1.0
25.00[a]	106.1	129.98	29.26	1.1
22.50[a]	180.5	134.98	48.81	0.90
20.00[a]	301.3	139.98	80.09	0.80
15.00[a]	653.7	149.98	169.0	0.60
12.50[a]	871.7	154.99	223.0	0.60

[a]Alpha particle detected.

$^4He(t,t)^4He$ 8.580 MeV

Scale Error = 0.40%

θ_{lab} (deg)	$\sigma(\theta)_{lab}$ (mb/sr)	$\theta_{c.m.}$ (deg)	$\sigma(\theta)_{c.m.}$ (mb/sr)	Rel. Error (%)
12.50	2812.0	21.90	933.9	0.40
15.00	2025.0	26.27	679.3	0.40
20.00	1102.0	34.96	375.3	0.40
25.00	562.3	43.60	200.2	0.40
30.00	268.9	52.17	99.81	0.40
35.00	138.5	60.65	54.07	0.49
40.00	98.71	69.01	40.93	0.49
45.00	95.01	77.24	42.26	0.52
50.00	91.59	85.30	44.18	0.46
55.00	78.65	93.16	41.60	0.71
35.00[a]	63.27	109.96	19.30	0.9
32.50[a]	40.25	115.00	11.93	0.9
30.00[a]	27.87	119.97	8.041	1.0
27.50[a]	32.59	124.97	9.181	1.1
25.00[a]	61.51	129.97	16.96	1.5
20.00[a]	219.6	139.98	58.37	0.70
15.00[a]	504.1	149.97	130.3	0.60
12.50[a]	670.7	155.01	171.6	0.60

[a]Alpha particle detected.

$^4He(t,t)^4He$ 8.790 MeV

Scale Error = 0.40%

θ_{lab} (deg)	$\sigma(\theta)_{lab}$ (mb/sr)	$\theta_{c.m.}$ (deg)	$\sigma(\theta)_{c.m.}$ (mb/sr)	Rel. Error (%)
12.50	2549.0	21.90	846.5	0.46
25.00	539.1	43.59	191.9	0.40
30.00	240.8	52.17	89.37	0.40
37.57	72.25	64.97	29.08	0.60
40.00	62.28	69.00	25.83	0.60
45.00	66.26	77.25	29.47	0.56
50.00	76.43	85.29	36.86	0.70
55.00	74.50	93.17	39.40	0.90
37.50[a]	88.85	104.96	27.99	1.0
35.00[a]	70.10	109.97	21.38	1.0
32.50[a]	51.82	114.97	15.36	1.1
30.00[a]	41.10	119.97	11.85	1.3
25.00[a]	76.25	129.97	21.02	1.3
20.00[a]	225.5	139.99	59.94	1.0
16.76[a]	388.0	146.50	101.2	0.90
15.00[a]	485.0	149.99	125.4	0.80
12.50[a]	638.1	154.99	163.2	0.70

[a]Alpha particle detected.

$^4He(t,t)^4He$ 3.980 MeV

Scale Error = 0.40%

θ_{lab} (deg)	$\sigma(\theta)_{lab}$ (mb/sr)	$\theta_{c.m.}$ (deg)	$\sigma(\theta)_{c.m.}$ (mb/sr)	Rel. Error (%)
12.50	2636.0	21.90	875.4	0.40
15.00	1932.0	26.27	648.1	0.40
20.00	1062.0	34.96	365.7	0.40
22.50	760.5	39.29	265.9	0.40
25.00	534.7	43.60	190.3	0.40
27.50	364.9	47.88	132.5	0.40
30.00	243.4	52.16	90.34	0.40
32.50	165.9	56.43	63.09	0.40
35.00	113.5	60.64	44.33	0.50
37.50	89.14	64.86	35.83	0.58
40.00	79.91	69.01	33.13	0.62
45.00	83.64	77.24	37.20	0.51
50.00	88.09	85.30	42.50	0.51
55.00	79.96	93.16	42.34	0.70
37.50[a]	89.40	104.96	28.16	1.1
35.00[a]	67.68	109.98	20.64	0.9
32.50[a]	46.06	114.96	13.65	1.0
30.00[a]	33.96	119.98	9.796	1.0
27.50[a]	39.36	124.97	11.09	1.6
25.00[a]	71.44	129.97	19.69	1.2
22.50[a]	138.4	134.98	37.41	1.0
20.00[a]	240.6	139.98	63.93	0.80
15.00[a]	534.0	149.98	138.1	0.70
12.50[a]	711.9	154.99	182.1	0.60

[a]Alpha particle detected.

$^4He(t,t)^4He$ 9.880 MeV

Scale Error = 0.40%

θ_{lab} (deg)	$\sigma(\theta)_{lab}$ (mb/sr)	$\theta_{c.m.}$ (deg)	$\sigma(\theta)_{c.m.}$ (mb/sr)	Rel. Error (%)
12.50	2023.0	21.91	671.6	0.40
15.00	1494.0	26.27	501.2	0.42
20.00	856.2	34.96	294.7	0.40
25.00	476.00	43.60	169.4	0.40
30.00	255.6	52.17	94.88	0.40
30.00	257.1	52.17	95.44	0.40
32.50	190.3	56.41	72.38	0.40
35.00	146.6	60.65	57.23	0.42
36.63	129.4	63.39	51.08	0.37
37.50	120.2	64.83	48.29	0.47
40.00	104.8	69.02	43.45	0.52
42.50	94.59	73.14	40.56	0.45
45.00	88.30	77.25	39.20	0.40
47.50	81.80	81.30	37.83	0.51
50.00	76.32	85.29	36.70	0.45
52.50	68.59	89.27	34.61	0.51
53.85	63.62	91.38	32.94	0.90
55.00	58.36	93.17	30.90	2.00
57.50	48.82	97.00	27.21	0.80
40.00[a]	73.11	99.96	23.85	0.61
35.05[a]	33.88	109.89	10.315	0.84
30.00[a]	9.024	119.97	2.863	1.2
25.00[a]	50.95	129.99	14.05	0.80
20.00[a]	188.0	139.98	49.96	0.80
15.00[a]	398.1	150.00	102.9	0.49
15.00[a]	398.3	150.00	103.0	0.50
12.50[a]	507.5	154.98	129.8	0.90

[a]Alpha particle detected.

$^4He(t,t)^4He$ 12.00 MeV

Scale Error = 0.40%

θ_{lab} (deg)	$\sigma(\theta)_{lab}$ (mb/sr)	$\theta_{c.m.}$ (deg)	$\sigma(\theta)_{c.m.}$ (mb/sr)	Rel. Error (%)
12.50	1187.0	21.91	393.9	0.40
15.00	988.6	26.27	331.5	0.40
20.00	685.7	34.97	235.9	0.40
25.00	432.7	43.61	154.0	0.40
30.00	256.7	52.18	87.85	0.40
35.00	117.7	60.66	45.93	0.50
40.00	71.78	69.02	29.76	0.60
45.00	67.50	77.26	30.02	0.56
50.00	71.61	85.31	34.54	0.51
45.00[a]	98.84	89.95	34.95	0.70
40.00[a]	78.79	99.97	25.70	0.80
35.00[a]	34.95	109.96	10.66	1.2
30.00[a]	15.92	119.96	4.591	2.0
25.00[a]	71.04	129.97	19.60	1.2
20.00[a]	195.6	139.97	51.99	1.0
15.00[a]	339.2	149.98	87.69	0.70
12.50[a]	433.8	154.90	103.3	0.70

[a]Alpha particle detected.

$^4He(t,t)^4He$ (15.00° lab) Tritons Detected

Scale Error = 0.40%

E_t (MeV)	$\sigma(\theta)_{lab}$ (mb/sr)	$\theta_{c.m.}$ (deg)	$\sigma(\theta)_{c.m.}$ (mb/sr)	Rel. error (%)
7.600	2728.0	26.26	915.3	0.40
7.800	2657.0	26.25	891.4	0.40
8.000	2529.0	26.26	848.4	0.40
8.200	2387.0	26.27	801.0	0.40
8.300	2311.0	26.27	775.5	0.40
8.391	2240.0	26.27	751.3	0.40
8.500	2136.0	26.26	716.7	0.40
8.580	2031.0	26.26	681.4	0.40
8.650	1888.0	26.27	633.3	0.40
8.700	1745.0	26.27	585.6	0.40
8.750	1720.0	26.27	576.9	0.40
8.800	1881.0	26.27	630.9	0.40
8.850	1971.0	26.27	661.2	0.40
8.900	1979.0	26.27	663.9	0.40
9.000	1924.0	26.27	645.5	0.40
9.100	1859.0	26.27	623.4	0.40
9.200	1809.0	26.27	606.9	0.40
9.400	1704.0	26.28	571.7	0.40
9.600	1608.0	26.28	539.2	0.40
9.844	1517.0	26.28	508.9	0.40
10.000	1446.0	26.27	484.8	0.40

$^4He(t,t)^4He$ (28.50° lab) Tritons Detected: Excitation Function

Scale Error = 0.40%

E_t (MeV)	$\sigma(\theta)_{lab}$ (mb/sr)	$\theta_{c.m.}$ (deg)	$\sigma(\theta)_{c.m.}$ (mb/sr)	Rel. error (%)
7.600	354.3	49.58	129.8	0.40
7.800	336.6	49.58	123.3	0.40
8.000	332.7	49.59	121.9	0.40
8.200	334.2	49.59	122.4	0.40
8.300	336.8	49.59	123.4	0.40
8.350	337.4	49.59	123.6	0.40
8.391	338.4	49.58	123.9	0.40
8.500	334.9	49.60	122.6	0.40
8.600	339.0	49.60	124.2	0.40
8.650	340.6	49.60	124.8	0.40
8.700	342.0	49.61	125.3	0.40
8.750	328.4	49.60	120.3	0.40
8.800	313.8	49.61	114.9	0.40
8.850	307.7	49.61	112.7	0.40
8.900	309.9	49.61	113.5	0.40
9.000	311.9	49.62	114.2	0.40
9.100	312.7	49.61	114.5	0.40
9.200	312.9	49.61	114.6	0.40
9.400	313.7	49.60	114.9	0.40
9.600	312.5	49.60	114.4	0.40
9.800	309.9	49.60	113.5	0.40
10.000	306.1	49.60	112.1	0.40

$^4He(t,t)^4He$ (40.00° lab) Tritons Detected

Scale Error = 0.40%

E_t (MeV)	$\sigma(\theta)_{lab}$ (mb/sr)	$\theta_{c.m.}$ (deg)	$\sigma(\theta)_{c.m.}$ (mb/sr)	Rel. Error (%)
7.600	26.92	69.00	11.16	0.90
7.800	37.09	69.01	15.38	0.90
8.000	53.86	69.01	22.34	0.80
8.200	69.97	69.00	29.01	0.75
8.300	77.95	69.01	32.32	0.75
8.391	82.71	69.01	34.29	0.75
8.500	90.92	69.01	37.70	0.70
8.580	99.61	69.01	41.31	0.70
8.650	105.9	69.01	43.93	0.70
8.700	103.2	69.01	42.78	0.70
8.750	76.02	69.01	31.52	0.75
8.800	61.39	69.01	25.46	0.75
8.850	66.97	69.01	27.77	0.70
8.900	71.44	69.01	29.62	0.70
9.000	81.24	69.02	33.68	0.65
9.100	87.82	69.02	36.42	0.65
9.200	91.55	69.02	37.95	0.65
9.400	98.13	69.02	40.69	0.65
9.600	102.0	69.02	42.28	0.60
9.800	103.0	69.02	42.70	0.60
10.000	105.6	69.02	43.76	0.60

$^4He(t,t)^4He$ (28.50° lab) Alphas Detected

Scale Error = 0.40%

E_t (MeV)	$\sigma(\theta)_{lab}$ (mb/sr)	$\theta_{c.m.}$ (deg)	$\sigma(\theta)_{c.m.}$ (mb/sr)	Rel. Error (%)
7.600	174.2	123.01	49.52	3.0
7.800	133.0	123.01	37.80	3.0
8.000	98.65	122.99	28.04	3.0
8.200	70.97	122.99	20.18	3.0
8.300	59.76	122.99	16.98	3.0
8.350	54.65	122.99	15.54	3.0
8.391	49.85	123.0	14.17	3.0
8.500	38.05	122.97	10.82	3.0
8.600	25.31	122.97	7.194	3.0
8.650	18.33	122.97	5.211	3.0
8.700	15.10	122.97	4.292	3.0
8.750	29.62	122.98	8.422	3.0
8.800	42.56	122.97	12.10	3.0
8.850	42.39	122.97	12.05	4.0
8.900	39.05	122.97	11.10	4.0
9.000	31.63	122.96	8.994	4.0
9.100	27.17	122.97	7.724	4.0
9.200	23.74	122.97	6.748	5.0
9.400	19.20	122.98	5.460	5.0
9.600	16.16	122.98	4.592	6.0
9.800	13.89	122.98	3.947	6.0
10.000	12.76	122.99	3.628	6.0

$^4He(t,t)^4He$ (15.00° lab) Alphas Detected

Scale Error = 0.40%

E_t (MeV)	$\sigma(\theta)_{lab}$ (mb/sr)	$\theta_{c.m.}$ (deg)	$\sigma(\theta)_{c.m.}$ (mb/sr)	Rel. error (%)
7.600	889.9	149.99	230.1	0.53
7.800	829.0	150.00	214.4	0.54
8.000	754.7	149.95	195.1	0.57
8.200	677.0	149.97	175.1	0.59
8.300	640.8	149.98	165.7	0.60
8.391	597.2	149.98	154.4	0.62
8.500	556.9	149.99	144.0	0.65
8.580	504.2	149.98	130.4	0.58
8.650	434.7	149.97	112.4	0.62
8.700	362.2	149.97	93.64	0.67
8.750	373.2	149.98	96.48	0.77
8.800	494.0	149.97	127.7	0.67
8.850	540.7	149.97	139.8	0.64
8.900	546.7	149.97	141.3	0.64
9.000	528.6	149.97	136.7	0.65
9.100	509.2	149.97	131.7	0.66
9.200	488.9	149.98	126.4	0.67
9.400	459.0	149.97	118.7	0.69
9.600	437.3	149.97	113.1	0.70
9.844	409.2	149.97	105.8	0.72
10.000	393.9	149.98	101.8	0.74